Science of the Total Environment 689 (2019) 366–380

Contents lists available at ScienceDirect

Science of the Total Environment

journal homepage: www.elsevier.com/locate/scitotenv

Continuous monitoring of lake dynamics on the Mongolian Plateau using all available Landsat imagery and Google Earth Engine

Yan Zhou [a,b,c], Jinwei Dong [a,b,*], Xiangming Xiao [d,e], Ronggao Liu [f], Zhenhua Zou [d], Guosong Zhao [a], Quansheng Ge [a,*]

[a] Key Laboratory of Land Surface Pattern and Simulation, Institute of Geographic Sciences and Natural Resources Research, Chinese Academy of Sciences, Beijing 100101, China
[b] University of Chinese Academy of Sciences, Beijing 100049, China
[c] School of Earth Sciences and Resources, China University of Geosciences, Beijing 100083, China
[d] Department of Microbiology and Plant Biology, Center for Spatial Analysis, University of Oklahoma, Norman, OK 73019, USA
[e] Ministry of Education Key Laboratory of Biodiversity Science and Ecological Engineering, Institute of Biodiversity Science, Fudan University, Shanghai 200438, China
[f] State key Laboratory of Resources and Environmental Information System, Institute of Geographic Sciences and Natural Resources Research, Chinese Academy of Sciences, Beijing 100101, China

HIGHLIGHTS

- Investigate interannual variations of lake areas and numbers on Mongolian Plateau (MP)
- Use all available Landsat images, a threshold-based algorithm, and GEE for lake mapping
- Shrinking lakes on MP recovered since 2009, with more drastic changes in Inner Mongolia
- Limited regions/lakes dominated variations of lake areas in Inner Mongolia and Mongolia

GRAPHICAL ABSTRACT

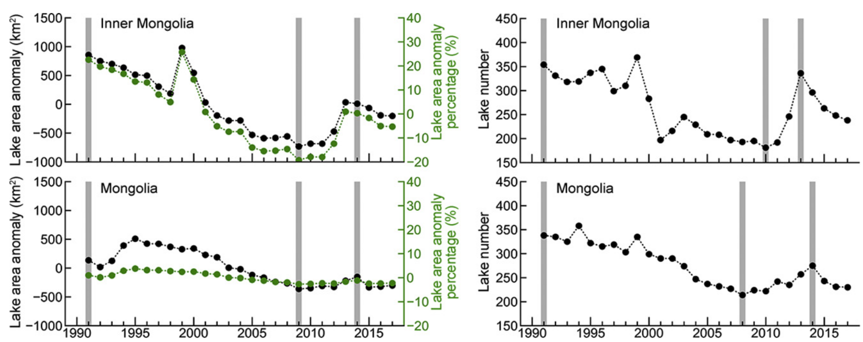

ARTICLE INFO

Article history:
Received 16 February 2019
Received in revised form 12 June 2019
Accepted 21 June 2019
Available online 24 June 2019

Editor: Ralf Ludwig

Keywords:
Lake dynamics
Mongolian Plateau (MP)
Google Earth Engine (GEE)
Landsat
Recovery
Drivers

ABSTRACT

Lakes are important water resources on the Mongolian Plateau (MP) for human's livelihood and production as well as maintaining ecosystem services. Previous studies, based on the Landsat-based analyses at epoch scale and visual interpretation approach, have reported a significant loss in the lake areas and numbers, especially from the late 1990s to 2010. Given the remarkable inter- and intra-annual variations of lakes in the arid and semi-arid region, a comprehensive picture of annual lake dynamics is needed. Here we took advantages of the power of all the available Landsat images and the cloud computing platform Google Earth Engine (GEE) to map water body for each scene, and then extracted lakes by post-processing including raster-to-vector conversion and separation of lakes and rivers. Continuous dynamics of the lakes over 1 km^2 was monitored annually on the MP from 1991 to 2017. We found a significant shrinkage in the lake areas and numbers of the MP from 1991 to 2009, then the decreasing lakes on the MP have recovered since circa 2009. Specifically, Inner Mongolia of China experienced more dramatic lake variations than Mongolia. A few administrative regions with huge lakes, including Hulunbuir and Xilin Gol in Inner Mongolia and Ubsa in Mongolia, dominated the lake area variations in the study area, suggesting that the prior treatments on these major lakes would be critical for water management on the MP. The varied drivers of lake variations in different regions showed the complexity of factors impacting lakes. While both natural and anthropogenic factors significantly affected lake dynamics before 2009, precipitation played increasingly important role for the recovery of lakes on the MP after 2009.

* Corresponding authors at: A11 Datun Road, Chaoyang District, Beijing 100101, China.
E-mail addresses: dongjw@igsnrr.ac.cn (J. Dong), geqs@igsnrr.ac.cn (Q. Ge).

https://doi.org/10.1016/j.scitotenv.2019.06.341
0048-9697/

1. Introduction

Lakes are primary water resources for people's livelihood as well as agricultural and industrial production on the Mongolian Plateau (MP), a typical arid and semi-arid region (Gao et al., 2017; O'Reilly et al., 2015). Meanwhile, some of these lakes are internationally important wetlands coupled with their surrounding surface runoff (e.g., Lake Hulun in Inner Mongolia of China, Lake Uvs in Mongolia). These lakes play an irreplaceable role in maintaining biodiversity by protecting threatened species and migratory waterfowls (e.g., Golden Eagle, White-headed Duck) (Liu et al., 2013; Tao et al., 2015), and provide essential supports for ecosystem services related to human wellbeing (Chen et al., 2012; Han et al., 2017; Li et al., 2017). However, due to the increasing pressure from human activities and climate change, substantial lake shrinkage and wetland degradation occurred in the past decades (Chang et al., 2015; Chen et al., 2018; Hou et al., 2017; Liu et al., 2017; Tao et al., 2015). The lake shrinkage brought considerable threats to the regional environment and ecosystems, including dust release, water salinization, and waterfowl decline (Hou et al., 2018; Liu et al., 2013; Ma et al., 2010; Wang et al., 2018). Given the potential negative effects of lake deterioration on the MP, monitoring lake changes on the entire plateau is of great significance to assess climate change impacts (Lu et al., 2011), and to protect regional ecosystems in such a typical arid and semi-arid region. However, existing efforts have been limited so far.

With the rapid development of remote sensing technology in the past several decades, satellite-based water body mapping has become a main approach to monitor water body changes (Chen et al., 2018; Hou et al., 2018; Huang et al., 2018; Rokni et al., 2015), which enables large-scale water resource monitoring particularly in remote and inaccessible mountain regions (Buchroithner and Bolch, 2015; Crétaux et al., 2011; Song et al., 2013; Song et al., 2014; Zhang et al., 2011). Among all the satellite sensors, Landsat family sensors have the longest satellite monitoring capability and medium spatial resolution (Chander et al., 2009; Hansen and Loveland, 2012; Ju and Roy, 2008; Wulder and Coops, 2014). Although there has been a series of researches on open surface water body mapping (Feyisa et al., 2014; Fisher et al., 2016; McFeeters, 1996; Xu, 2006; Yamazaki et al., 2015), only a few studies had been conducted on time series analysis of lake dynamics using historical Landsat imagery on regional scales, especially in a region (e.g., the MP) with fragile ecosystems which is sensitive to climate change. Liu et al. (2013) researched the decadal changes of lakes over 1 km^2 in the semi-arid steppe region in northern China from 1975 to 2009, and found a general reduction in the water areas of lakes since the 1990s. Moreover, they found the regional-scale lake shrinkage and desiccation in the semiarid region of China was initially caused by climate drying. Tao et al. (2015) investigated the changes of lakes (>10 km^2) on the MP over nine periods (every three, four, or five years for a period) from 1970s to 2010 using single period cloud-free Landsat images collected in Junes to Septembers of each period, and found a rapid loss of lake water areas on the plateau after the mid-1990s, with a doubled rate of decreases in Inner Mongolia of China than that in Mongolia. Furthermore, they found precipitation was the main driver for the lake loss in Mongolia while coal mining and irrigation were the major drivers for lake deterioration in Inner Mongolia from the 1980s to 2010. On the basis of the lake data (MP, 1976–2010) from Tao et al. (2015), Zhang et al. (2017) extended the study period by generating the lake map of the MP for the year 2013, and discussed the area changes of lakes (>10 km^2) on the MP during 1976–2013. Moreover, they found that the drier climate since 1998 could have been the dominant driver of lake shrinkage on the MP.

All the previous studies related to the lake dynamics on the MP mentioned above were carried out by sparse temporal dynamic analyses. However, due to the rapid inter- and intra-annual variations of climate on the MP, epoch-based dynamic analyses could miss important interannual variation information (e.g., turning points) and seasonality of lake dynamics (L. Chen et al., 2014). In addition, lake investigation in the previous studies mainly focused on large lakes over 10 km^2 (Tao et al., 2015; Zhang et al., 2017), and the climatic and anthropogenic driver analyses of lake changes were conducted based on these large lakes. Because the widely distributed smaller lakes under 10 km^2 on the MP were more vulnerable to regional climate and human activities (Zhang et al., 2017), the driver analyses without considering these lakes could omit some important mechanisms of climatic effects on lake changes. Last but not least, previous studies all reported that lakes were shrinking on the MP before 2010, while it is still unclear whether the lake shrinkage continued in the recent decade.

In view of the above-mentioned issues, improved understanding of lake variations and their drivers could be considered from the following perspectives: 1) continuous long-term lake monitoring at inter- or intra-annual scale. Annual water body dynamics have been detected in previous studies such as the yearly and monthly global water body maps at 30-m resolution from 1984 to 2015 produced by the Joint Research Center (JRC) of the European Commission (Pekel et al., 2016) and the annual water body maps for the United States from 1984 to 2016 (Zou et al., 2018). However, continuous monitoring of annual lake dynamics needs further analyses including extraction of lakes from water body maps; 2) climatic and anthropogenic driver analyses based on the continuous lake monitoring could provide a more promising understanding than that based on epoch-based analyses. For example, Zou et al. (2017) conducted the driver analyses of annual water body dynamics in the Oklahoma state of the United States, and found that precipitation had statistically positive effects on water body area, while temperature, and surface water withdrawals for public water supply and agricultural irrigation had negative effects; 3) in addition to the big lakes over 10 km^2, smaller lakes (<10 km^2) should also be considered in lake dynamic analyses (Liu et al., 2013; Zou et al., 2017; Zou et al., 2018).

In this study, we aimed to draw a whole picture of the annual lake (>1 km^2) dynamics on the MP from 1991 to 2017. In doing so, the objectives of this paper are mainly three parts: (1) to extract annual lake maps on the MP from the water body maps which was generated by using a water and vegetation indices-based water body mapping algorithm, all the available Landsat images, and the cloud computing platform Google Earth Engine (GEE); (2) to investigate the areas and numbers of the lakes over 1 km^2 on the MP, and then compare the results with those according to the JRC water body map datasets (Pekel et al., 2016); (3) to investigate the driving factors of lake changes on the MP including both natural and anthropogenic factors. This study provides an unprecedented lake dataset for the MP since 1991 (see Text S1, Fig. S1, Tables S1 and S2 for detailed information), and also expects to provide updated understanding of the interannual dynamics of lakes on the MP and its drivers, which would contribute to regional water resource management and protection.

2. Materials and methods

2.1. Study area

The Mongolian Plateau (MP) geographically includes the Inner Mongolia Autonomous Region of China and the Mongolian People's Republic, with an area of approximately 2.7 million km^2 at an average elevation higher than 1500 m, and a population of about 28 million (Bao et al., 2014; John et al., 2018; Tao et al., 2015). Because of its large spatial domain and high elevation, the plateau and its surroundings play a vital role in the Earth's climate system through their unique atmosphere interactions (Sha et al., 2015). The MP is one of the most sensitive regions in the world to climate change (J. Chen et al., 2014), and rapid weather dynamics are the greatest characteristic of its climate (Zhang et al., 2017). The plateau has been experiencing a process of higher warming rate than the rest regions in the world over the past decades (Zhang et al., 2017). Specifically, both Inner Mongolia and

Mongolia include desert, grassland, and forest biomes, with distinctive eco-climatic zones (John et al., 2013). Both regions exhibit significant variations in biophysical conditions (e.g., climates, biomes) from east to west, resulting in distinct climates, ecosystems, and livelihoods (J. Chen et al., 2014). In addition, political systems and socioeconomic development conditions varied substantially in Inner Mongolia and Mongolia (J. Chen et al., 2014). The economy of Inner Mongolia is dominated by industry while that of Mongolia is dominated by animal husbandry, which caused different land use and landscape patterns (J. Chen et al., 2014; John et al., 2013).

2.2. Landsat images

All the Landsat TM, ETM+, and OLI Collection 1 Tier 1 surface reflectance data in the study area from 1991 to 2017 (~150,000 images, >100 terabytes of data) which were originally from the United States Geological Survey (USGS) were used to identify open surface water bodies and lakes. All these images were derived from the Google Earth Engine (GEE) (https://earthengine.google.org/), which is a cloud-based computation platform and provides high-performance computing capability and abundant geospatial datasets from the National Aeronautics and Space Administration (NASA) as well as other sources (Gorelick et al., 2017; Patel et al., 2015; Zurqani et al., 2018). The Landsat Collection 1 Tier 1 images have been conducted geometric and atmospheric correction, as well as cross-calibration among the different sensors (Dwyer et al., 2018; Wulder et al., 2016). This study did not cover the previous period (1984–1990) due to the limited Landsat data availability and quality across the entire MP (Fig. 1a and b). For each image, the cloud, cloud shadow and snow pixels were removed by using the data quality layer from a cloud masking method named CFmask, which works well and is suitable for preparing Landsat data for change detection (Zhu and Woodcock, 2014). Terrain shadows were considered and removed as well by using the solar azimuth and zenith angles from Landsat images and the digital elevation model from Shuttle Radar Topography Mission (Fig. S2). All the remaining pixels were considered as good-quality Landsat observations that can be used for open surface water body mapping. The pixels with zero good-quality Landsat observation in a year account for 24.49% on average during 1984–1990 and 0.00% during 1991–2017 (Fig. 1c). All the Landsat pixels within the MP had a number of total observations ≥511 and good-quality observations ≥75 in the last 27 years (Fig. 1d and e). Finally, annual cloud- and snow-free image collections comprising all Landsat TM, ETM+, and OLI images in the study area were generated based on GEE (Nyland et al., 2018).

2.3. Water body detection and validation

Open surface water bodies can be detected by using the relationships between water and vegetation indices, and previous studies have performed water body change analyses based on time series Landsat images and indices- and threshold-based water body mapping algorithms (Chen et al., 2017; Zou et al., 2017; Zou et al., 2018). The water and vegetation indices including modified Normalized Difference Water Index (mNDWI), Enhanced Vegetation Index (EVI), and Normalized Difference Vegetation Index (NDVI) were used in water body mapping in this study (Fig. 2 and Text S2). These water and vegetation indices were calculated by using the cloud- and snow-free Landsat TM, ETM+, and OLI surface reflectance images based on the following spectral bands and equations:

$$mNDWI = \frac{\rho_{Green} - \rho_{SWIR1}}{\rho_{Green} + \rho_{SWIR1}} \quad (1)$$

$$NDVI = \frac{\rho_{NIR} - \rho_{Red}}{\rho_{NIR} + \rho_{Red}} \quad (2)$$

$$EVI = 2.5 \times \frac{\rho_{NIR} - \rho_{Red}}{1.0 + \rho_{NIR} + 6.0\rho_{Red} + 7.5\rho_{Blue}} \quad (3)$$

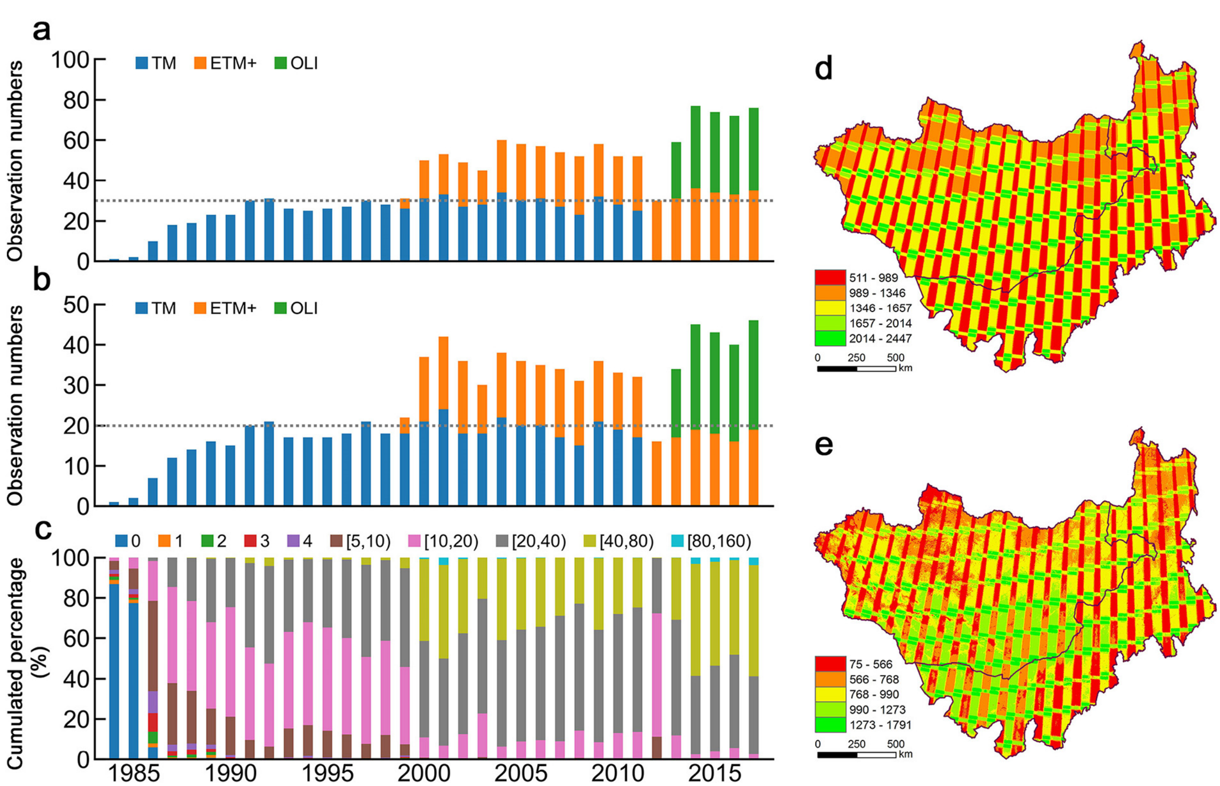

Fig. 1. Statistics of Landsat observations across the entire Mongolian Plateau (MP). The yearly average number of total (a) and good-quality (b) Landsat observations of the MP from 1984 to 2017. (c) Cumulative percentage of Landsat pixels within the MP with good-quality observation numbers of 0, 1, 2, 3, 4, [5, 10), [10, 20), [20, 40), [40, 80), and [80, 160), respectively. Spatial distributions of the total (d) and good-quality (e) Landsat observations within the MP from 1991 to 2017.

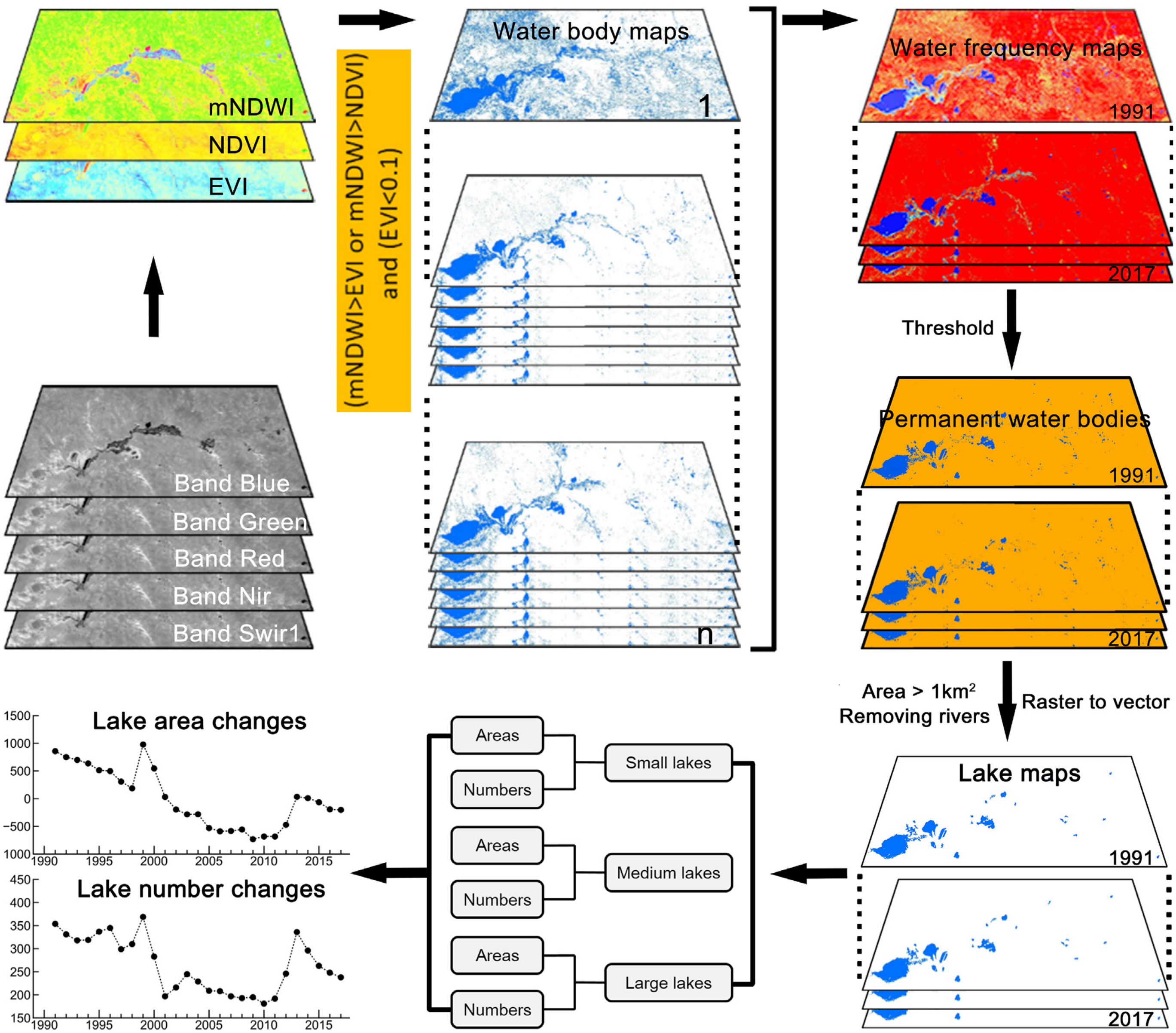

Fig. 2. Procedures of continuous monitoring of lake dynamics on the MP from 1991 to 2017 by using all the good-quality observations from Landsat 5 TM, Landsat 7 ETM+, and Landsat 8 OLI surface reflectance images, including the calculations of water and vegetation indices, water body mapping based on each scene, generations of annual water frequency maps, permanent water body maps and lake maps, and investigations of annual lake areas and numbers.

where ρ_{Blue}, ρ_{Green}, ρ_{Red}, ρ_{NIR}, and ρ_{SWIR1} are the surface reflectance values of Bands blue (0.45–0.52 μm), green (0.52–0.60 μm), red (0.63–0.69 μm), near-infrared (NIR) (0.77–0.90 μm) and shortwave-infrared-1 (SWIR1) (1.55–1.75 μm) in the Landsat TM, ETM+, and OLI sensors. A criterion mNDWI>EVI or mNDWI>NDVI was used to identify the pixels which show stronger water signal than vegetation signal. EVI < 0.1 can ensure that the vegetation pixels or the mixed pixels of water and vegetation were removed. Therefore, only those pixels meet the criteria [(mNDWI>EVI or mNDWI>NDVI) and (EVI < 0.1)] were classified as water body pixels while other pixels were classified as non-water pixels. The open surface water body mapping algorithm with analyses of time series Landsat images has been reported in our previous studies (Zou et al., 2017; Zou et al., 2018). For each Landsat pixel within the MP, its water frequency in a year was calculated by using Eq. (4):

$$F(y) = \frac{1}{N_y}\sum_{i=1}^{N_y} w_{y,i} \times 100\% \qquad (4)$$

where F is the water frequency of the pixel, y is the specified year, N_y is the number of total Landsat observations of the pixel in that year, $w_{y,i}$ denotes whether one observation of the pixel is water, with one indicating water and zero indicating non-water. Annual water frequency maps of the MP were generated by the annual water frequencies of all Landsat pixels (Fig. 2) After setting a certain threshold, water body areas were derived from the annual water frequency maps and they are varied according to different threshold values (Fig. 3a). We compared the water body areas of the MP using different frequency thresholds from our datasets with the permanent water body areas from the JRC datasets, and found a good agreement of the total area and interannual variability when the frequency threshold of our datasets was set to 0.75 (Fig. 3a). A permanent water surface is under water throughout the year (Pekel et al., 2016). Fig. 3b–e showed the water body maps of the MP and their zoom-in views in 2015 from our datasets with the frequencies ≥0.75 and the permanent water body maps from JRC datasets. Similar spatial distributions of surface water bodies in both our datasets and the JRC datasets could be found. Thus, water pixels with annual water frequencies ≥0.75 were extracted as permanent water bodies in this study (Fig. 3, and Text S3), which was consistent with our previous study (Zou et al., 2017; Zou et al., 2018).

We used the random sampling approach and ground truth data from Google Earth for the validation. A total of 1600 random regions of interest (100 m radius circles), equal to roughly 83,000 Landsat pixels, across the entire MP were visually interpreted in the Google Earth to validate the results. The detailed validation approach can be found in the supplemental document (Text S2 and Fig. S3). The results showed an overall accuracy of 96.41% with a kappa coefficient of 0.93 (Table S3). The data of lake surface height was used to provide additional verification of the results, which were derived from the global 10-day lake/reservoir surface height products from the United States Department of Agriculture's Foreign Agricultural Service (USDA-FAS, https://ipad.fas.usda.gov/cropexplorer/global_reservoir/) (see Text S4 for detailed description).

2.4. Lake extraction from water body maps

We converted the annual permanent water body maps from raster to vector format, which allowed us to further calculate the sizes of individual lakes. Then, the small water bodies (<1 km^2) were removed via filtering by area, and remaining rivers were checked and removed by referring to the very high spatial resolution images in Google Earth (Text S3). To better understand the changes in lakes, we divided the lakes into three categories according to their sizes: small (1–10 km^2), medium (10–50 km^2), and large lakes (>50 km^2) referring to (Tao et al., 2015). All the following statistical analyses were based on these three categories. The same analyses were conducted to process the annual permanent water body maps from JRC (Pekel et al., 2016).

2.5. Attribution analyses of lake dynamics

We considered both climate change and anthropogenic activities for the attribution analyses of interannual lake dynamics since 1991, including annual mean temperature (AMT), annual precipitation (AP) as measures of regional climate, grazing, coal mining, and irrigation as indicators of anthropogenic activities (Tao et al., 2015). The surface air temperature and precipitation data were derived from the University of East Anglia Climatic Research Unit (CRU TS V4.01) datasets (http://www.cru.uea.ac.uk/data/). The AMT was calculated by averaging monthly data from January to December in the same year (Text S5), while the AP was accumulated with monthly precipitation from January to December in the previous year due to the hysteresis of precipitation effects. The grazing (number of goats and sheep), coal mining (annual coal production), and irrigation (area of irrigated croplands) data of Inner Mongolia were obtained from *Inner Mongolia Statistical Year Book*, while the corresponding data of the Hulunbuir City and Xilin Gol League were collected from *Hulunbuir Statistical Year Book* and *Xilin Gol Statistical Year Book*. Additionally, those data of Mongolia were derived from the United States Energy Information Administration (http://www.indexmundi.com) and the Food and Agriculture Organization of the United Nations database (http://faostat.fao.org). To determine the possible driving factors of lake changes, we performed multiple linear regression analysis with software SPSS V20 using the "stepwise" method to select explanatory variables.

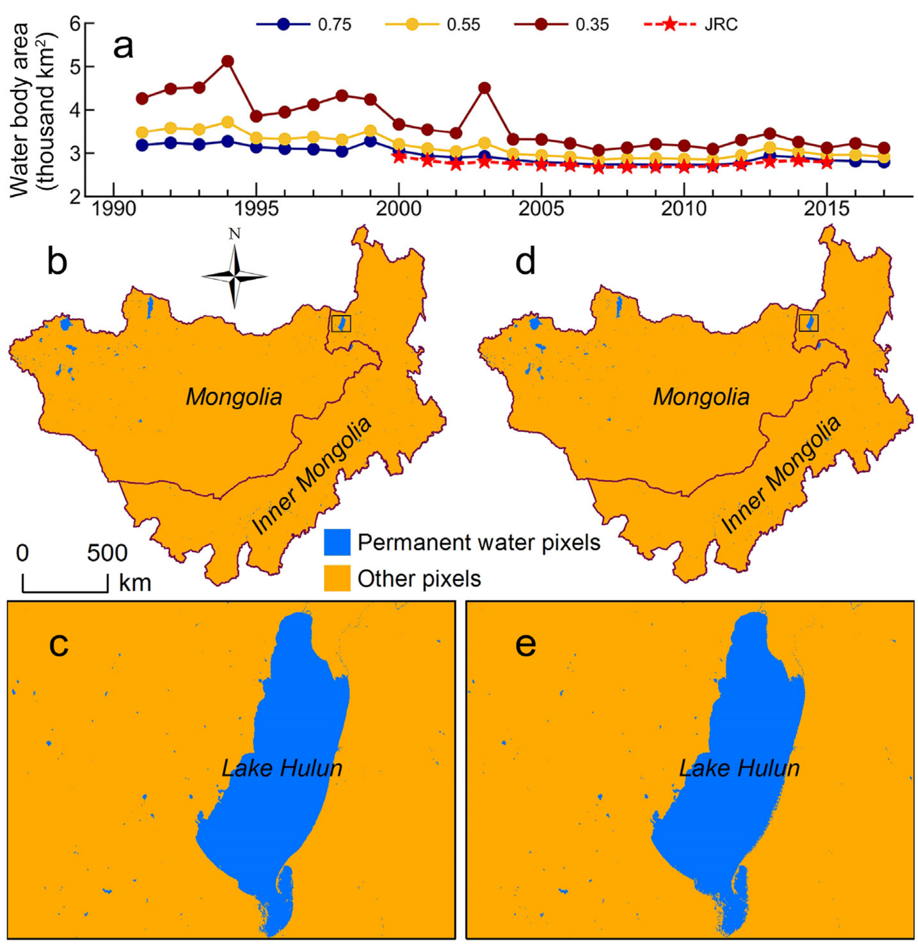

Fig. 3. Water body areas using different frequency thresholds and permanent water body maps of the MP. (a) Total water body area of all Landsat pixels within the MP with water frequencies ≥0.35, ≥0.55, and ≥0.75, respectively, in our datasets; and the permanent water body areas from the JRC datasets during 2000–2015. Water body maps of the MP in 2015 and their zoom-in views of Lake Hulun in Inner Mongolia from our datasets with frequencies ≥0.75 (b and c) and JRC permanent water body datasets (d and e), respectively.

3. Results and discussion

3.1. Changes in lakes >1 km^2 in Inner Mongolia and Mongolia from 1991 to 2017

Based on the statistical analyses on the interannual variations of both areas and numbers of lakes >1 km^2, we found that the entire MP experienced a significant decrease in lakes from 1991 to circa 2009 and then followed by a recovery process since circa 2009 (Fig. 4a and b). Both Inner Mongolia and Mongolia experienced similar trends, but Inner Mongolia showed more drastic changes than Mongolia (Fig. 4c–f). That was proved by both our generated maps as well as the results from JRC (2000–2015), and the JRC-based analyses before 2000 were not conducted due to the limited data availability (see Fig. S4 for more justification). Specifically, the difference was that the area anomaly ratio ranged from −20% below to 30% above the average in Inner Mongolia while it was relatively stable (−10%–10%) in Mongolia, which clearly showed the lakes in Mongolia were much more stable than that in Inner Mongolia (Fig. 4c and e). In addition, the results of clustering analyses according to the interannual variations of lake areas on the MP also showed that more rapid shrinkages of lakes occurred in Inner Mongolia than Mongolia (see Text S6, Fig. S5, Tables S4–S6 for details). Note that both lake areas and numbers in Inner Mongolia and Mongolia showed a slight decrease again since 2013 (Fig. 4c–f).

According to the variation trends of lakes in Inner Mongolia and Mongolia in Fig. 4, we selected the start year of 1991 and the two turning points of the years 2009 and 2013 for the analyses in different periods (Fig. 5). The total water surface area of lakes >1 km^2 in Inner Mongolia shrank greatly from 4660.6 km^2 in 1991 to 3071.4 km^2 in 2009 with a huge decrease of 1589.2 km^2 or 34.1%, from 22.6% above to 19.2% below its multi-year average (3802.8 km^2) during 1991–2017 (Table 1). However, an abrupt increase in lake areas and numbers during 1998–1999 can be seen in Inner Mongolia (Fig. 4c and d), which was mainly caused by the increase in lake areas and numbers in the Hulunbuir City and Xilin Gol League (Fig. 6a and b). Out of the decreased lake areas, the small, medium, and large lakes accounted for 21.1%, 11.2%, and 67.7%, respectively. Then, the total lake area gradually increased from 2009 to 2013 with an increase of 766.2 km^2 or 24.9%, from 3071.4 km^2 in 2009 to 3837.6 km^2 in 2013, which was 19.2% below and 0.9% above to the mean value (Table 1). The small, medium and large lakes contributed 33.6%, 34.8% and 31.6%, respectively, to the lake area growth.

As for Mongolia, the total area of lakes over 1 km^2 decreased from 13,606.0 km^2 in 1991 to 13,108.6 km^2 in 2009 with a smaller decrease (497.4 km^2 or 3.7%) compared to Inner Mongolia (1589.2 km^2 or 34.1%) (Table 1), that was, from 1.0% above to 2.7% below the 27-year average area (13,470.3 km^2). Note that the total lake area in Mongolia was much larger than that in Inner Mongolia, therefore, the lake dynamics was much milder than that in Inner Mongolia. Among the decreased water body extent from 1991 to 2009, the small, medium and large lakes accounted for 53.6%, 22.6%, and 23.8%, respectively. From 2009 to 2013, the lake areas of Mongolia experienced a smaller increase (142.1 km^2 or 1.1%) compared to the remarkable increases in Inner Mongolia (766.2 km^2 or 24.9%) (Table 1).

The average decreasing rates of lakes (88.3 km^2/yr and 9 lakes/yr) in Inner Mongolia during 1991–2009 was greater than those (27.6 km^2/yr and 6 lakes/yr) in Mongolia during the same period, which indicated that a larger proportion loss of lakes on the MP during 1991–2009 happened in Inner Mongolia, consistent with the previous study (Tao et al., 2015).

In terms of the changes in lake numbers, both regions showed similar trends to that of the area. Specifically, the number of lakes over

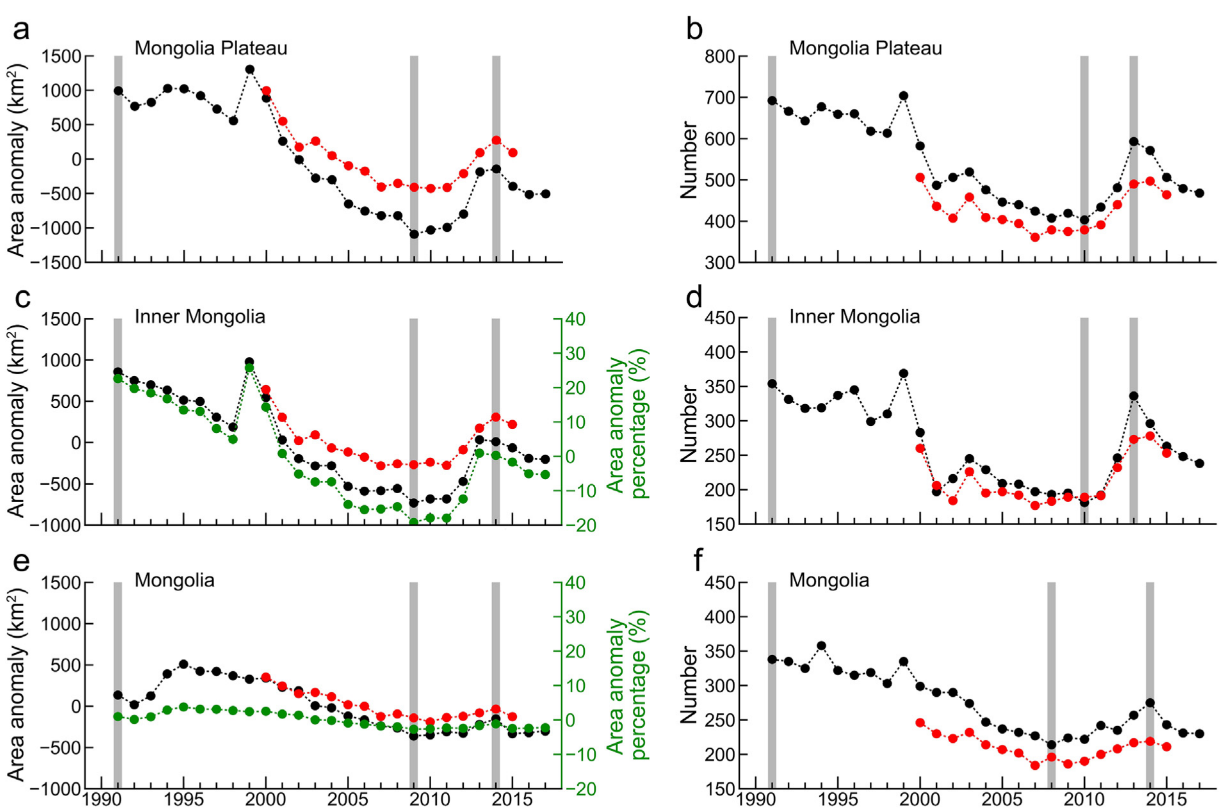

Fig. 4. Interannual variations of lakes on the MP from 1991 to 2017. Area and number variations of lakes on the MP (a and b), Inner Mongolia (c and d) and Mongolia (e and f) from 1991 to 2017. The black dotted lines show the changing trends of lakes on the MP from 1991 to 2017 based on the annual water frequency maps generated in this study. The red dotted lines show the variation trends of lakes on the MP from 2000 to 2015 based on the annual permanent water body maps from JRC. The grey bars show the start and turning points of lake changes on the MP from 1991 to 2017. More information about lake dynamics of the MP is shown in Table 1. (For interpretation of the references to colour in this figure legend, the reader is referred to the web version of this article.)

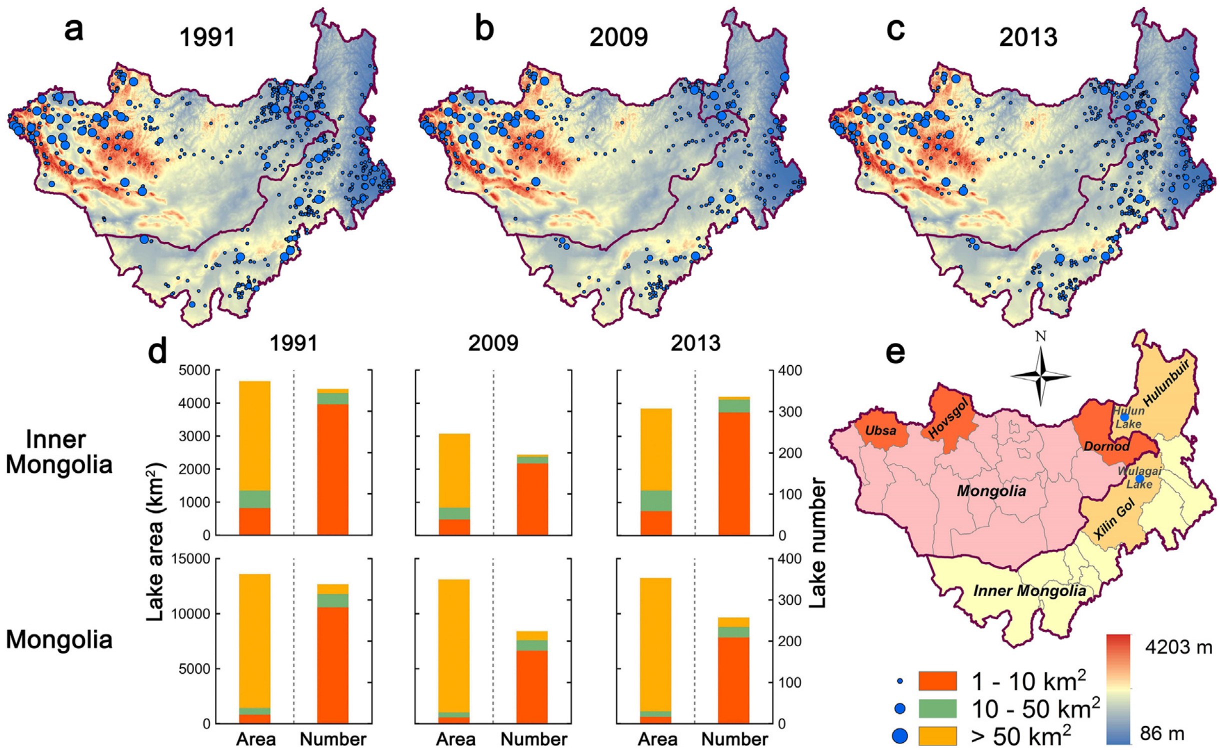

Fig. 5. Spatial distribution of different sizes of lakes on the MP in 1991 (a), 2009 (b), and 2013 (c). (d) The bar graphs at the bottom show the area (km^2) and number of small (orange), medium (green), and large lakes (yellow) in Inner Mongolia and Mongolia in 1991, 2009 and 2013. (e) Locations of the Hulunbuir City and Xilin Gol League of Inner Mongolia, the Aymags of Ubsa, Hovsgol and Dornod of Mongolia, as well as Lake Hulun and Lake Wulagai in the Hulunbuir City and Xilin Gol League, respectively. More information about the spatial distribution of lakes on the MP is shown in Figs. S1 and S6, Tables S1 and S2. (For interpretation of the references to colour in this figure legend, the reader is referred to the web version of this article.)

1 km^2 decreased greatly from 354 in 1991 to 195 in 2009 in Inner Mongolia, while this number decreased significantly from 338 in 1991 to 224 in 2009 in Mongolia (Table 1). Among the 159 (114) decreased lakes in Inner Mongolia (Mongolia), 143 (105) of them were small lakes, while 11 (7) were medium ones and 5 (2) were large ones (Table 1). Then the number increased rapidly from 195 (224) detected in 2009 to 336 (257) in 2013 in Inner Mongolia (Mongolia); among the 141 (33) increased lakes, 124 (32) of them were small lakes while 15 (0) were medium ones and 2 (1) was large ones (Table 1).

3.2. Lake changes in different administrative regions of Inner Mongolia and Mongolia

Given the more remarkable changes in Inner Mongolia, we analyzed lake dynamics for each administrative region in Inner Mongolia. We found that lake changes in the Hulunbuir City and Xilin Gol League experienced maximum lake dynamics of the entire Inner Mongolia, which was shown by the consistent changing trends between the two regions and the entire Inner Mongolia, as well as the dominant lake

Table 1
Detailed information on changes in the areas and numbers of lakes over 1 km^2 on the MP during the two periods of 1991–2009 and 2009–2013.

	Lakes in 1991		Lakes in 2009		Lakes in 2013		Lake changes (1991–2009)				Lake changes (2009–2013)			
Lake class	Num.	Area (km^2)	Num.	Area (km^2)	Num.	Area (km^2)	Num. of decreased lakes	ΔNum (%)	ΔArea (km^2)	ΔArea (%)	Num. of increased lakes	ΔNum (%)	ΔArea (km^2)	ΔArea (%)
Inner Mongolia														
1–10 km^2	317	816.7	174	480.8	298	738.0	143	−45.1	−335.9	−41.1	124	71.3	257.2	53.5
10–50 km^2	27	534.6	16	356.6	31	623.2	11	−40.7	−178.0	−33.3	15	93.8	266.6	74.8
>50 km^2	10	3309.3	5	2234	7	2476.4	5	−50.0	−1075.3	−32.5	2	40.0	242.4	10.9
All lakes	354	4660.6	195	3071.4	336	3837.6	159	−44.9	−1589.2	−34.1	141	72.3	766.2	24.9
Mongolia														
1–10 km^2	282	831.8	177	565.4	209	626.7	105	−37.2	−266.4	−32.0	32	18.1	61.3	10.8
10–50 km^2	32	585.2	25	472.7	25	493.4	7	−21.9	−112.5	−19.2	0	0	20.7	4.4
>50 km^2	24	12,189.0	22	12,070.5	23	12,130.6	2	8.3	−118.5	−1.0	1	4.5	60.1	0.5
All lakes	338	13,606.0	224	13,108.6	257	13,250.7	114	−33.7	−497.4	−3.7	33	14.7	142.1	1.1
Whole plateau														
1–10 km^2	599	1648.5	351	1046.2	507	1364.7	248	−41.4	−602.3	−36.5	156	44.4	318.5	30.4
10–50 km^2	59	1119.8	41	829.3	56	1116.6	18	−30.5	−290.5	−25.9	15	36.6	287.3	34.6
>50 km^2	34	15,498.3	27	14,304.5	30	14,607.0	7	−20.6	−1193.8	−7.7	3	11.1	302.5	2.1
All lakes	692	18,266.6	419	16,180.0	593	17,088.3	273	−39.5	−2086.6	−11.4	174	41.5	908.3	5.6

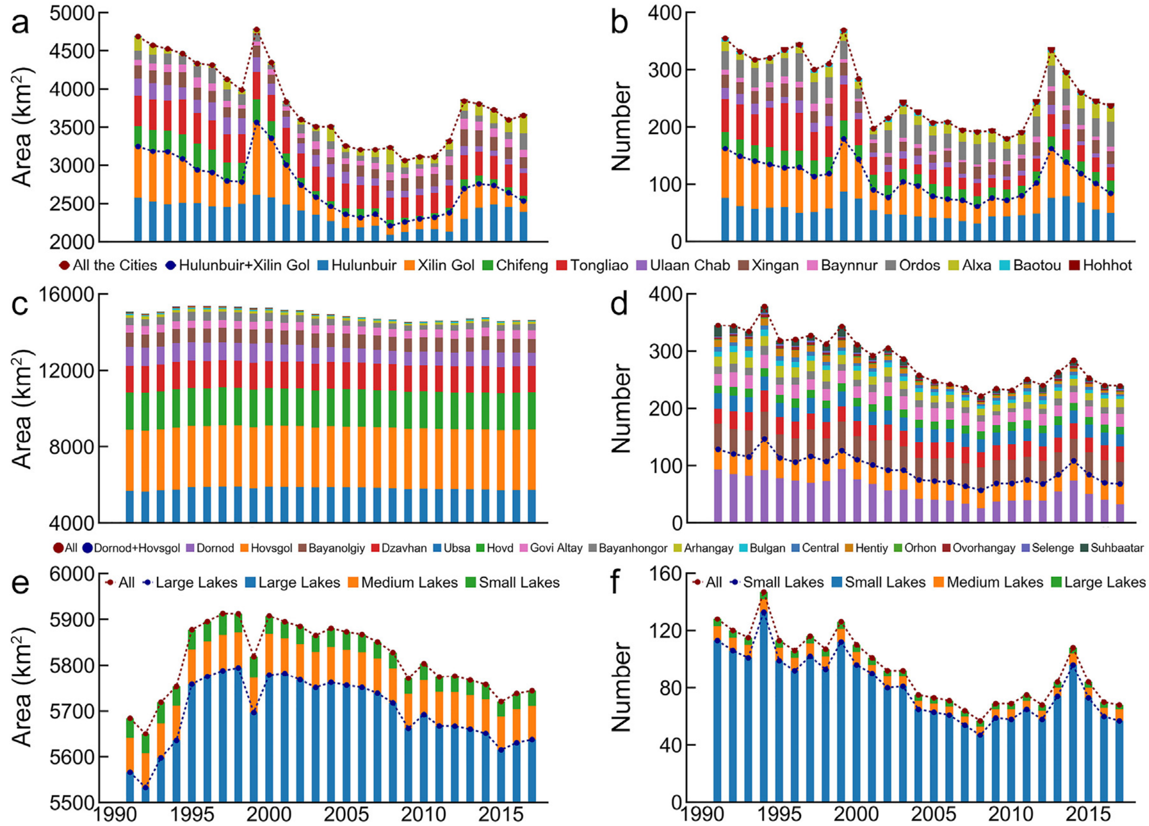

Fig. 6. Interannual variations of lake areas and numbers in Inner Mongolia and Mongolia during 1991–2017. Area and number composites of lakes in different administrative regions of Inner Mongolia (a and b) and Mongolia (c and d). Area composites of varied sizes of lakes in the Ubsa Aymag (e) and number composites of varied sizes of lakes in the Dornod Aymag and Hovsgol Aymag (f).

areas (60.0%) and numbers (57.6%) (Fig. 6a and b). Among the decreased water body extent of 1589.2 km^2 in entire Inner Mongolia from 1991 to 2009, the Hulunbuir City and Xilin Gol League accounted for 452.4 km^2 (28.5%) and 540.0 km^2 (34.0%), respectively. Among the total increased lake area of 766.2 km^2 from 2009 to 2013 in Inner Mongolia, the Hulunbuir City contributed 169.4 km^2 (22.1%) while the Xilin Gol League contributed 270.2 km^2 (35.3%). In terms of changes in lake numbers, among the decreased 159 lakes during 1991–2009, 33 lakes (20.8%) happened in Hulunbuir while 53 lakes (33.3%) happened in Xinlin Gol. And among the increased 141 lakes from 2009 to 2013, Hulunbuir and Xilin Gol occupied 33 (23.4%) and 53 (37.6%), respectively.

Compared to Inner Mongolia, Mongolia showed much milder lake dynamics (Fig. 4e and f). However, we also found the lake dynamics in Mongolia were mainly dominated by one or two provinces (Aymags). Specifically, the Ubsa Aymag possesses the largest lake area among all the provinces of Mongolia (Fig. 6c), which dominated the lake area variations of the country. It is notable that lake areas in Mongolia showed an increasing trend before 1995 (Figs. 4e and 6c), while the lake numbers declined during the same period (Figs. 4f and 6d). It was mainly caused by the area increase in large lakes in the Ubsa Aymag (Text S7, Fig. 6c and e). Lakes in the Dornod Aymag and Hovsgol Aymag played a leading role in lake number changes in Mongolia, as a large number of small lakes were distributed in the two regions (Figs. 3 and 4f). It was obvious that the variations in the lake numbers of the two provinces were consistent with that of the whole country (Fig. 6d and f).

3.3. Changes of Lake Hulun and Lake Wulagai in Inner Mongolia

We further found that the lake area decrease in the Hulunbuir City during 1991–2009 was mainly caused by the shrinkage of Lake Hulun, while that of the Xilin Gol League was caused by the shrinkage of Lake Wulagai. Fig. 7 showed the critical role of the two largest lakes in dominating the variations of lakes in Inner Mongolia. Lake Hulun is the largest lake in Northeast China and the fifth largest inland freshwater lake in China, which located in a semi-arid region in the northeast part of Inner Mongolia, close to the borders of China, Russia, and Mongolia (Cai et al., 2016; Lü et al., 2016). The lake sustains vast areas of unique wetlands which provide habitats for numerous wildlife, including many species of fish and endangered migratory birds (e.g., bustard, golden eagle) (Cai et al., 2016; Gao et al., 2017; Ke, 2016). However, the lake area continued to decline by approximately 535 km^2 since 2000, from 2282 km^2 in 2000 to 1747 km^2 in 2012, at an incredible decreasing rate of 44.6 km^2/yr (Fig. 8a). The decreased area of Lake Hulun (514 km^2) from 1991 to 2009 was larger than the total decreased water body extents in Hulunbuir City (452 km^2). That suggested there were other growing lakes offsetting the decrease of lake area in the city.

The northeastern and southern parts of Lake Hulun declined most obviously, and the northeastern part of the lake completely disappeared in 2005 from 171 km^2 originally in 1991 (Fig. 8a). The southern part of Lake Hulun gradually declined since 2006, and the water body then completely disappeared in 2012 (Fig. 8a). The convex part in the south of Lake Hulun was separated from the main water body in 2008 and then recovered in 2014 (Fig. 8a), which has been reported in the previous study (Wan et al., 2016). The variations of the annual water surface area of Lake Hulun were consistent with that of the annual average height of lake surface during 1993–2017, albeit the lack of lake surface height data before 1993 (Fig. 8b). The same consistency also happened in the other three big lakes, including Lake Har, Lake Dorgon, and Lake Khovsgol (Fig. S7), which provided additional evidence to verify the accuracy of the water body maps produced in this study.

Lake Wulagai, also named Wulagai Gaobi, located in the Xilin Gol League, is another big and saltwater lake playing an important role in the whole region (Li et al., 2013; Yu et al., 2014). Together with the

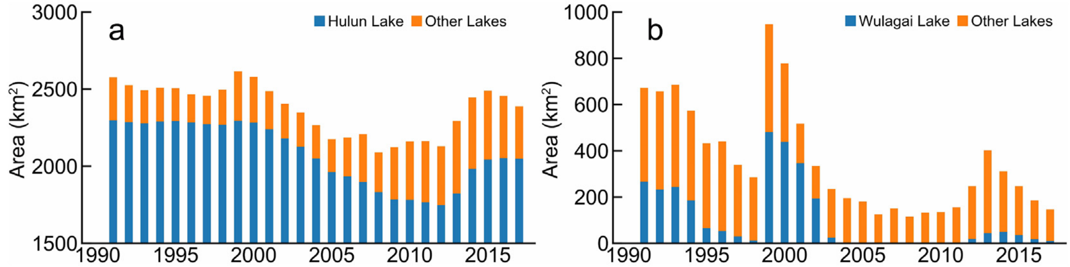

Fig. 7. The area composites of lakes in the Hulunbuir City (a) and Xilin Gol League (b) of Inner Mongolia.

Wulagai River, they formed a vast marsh which was an important habitat of a variety of precious migratory waterfowls (e.g., swan, red-crowned crane) in the past decades. However, the water volume of the lake continued to decline since 1991 and nearly dried up in 1998 (Fig. 9). There was a great jump in the water body extent of the lake in 1999 (even beyond the lake area in 1991); however, the lake started to decrease again after 1999 and completely dried up in 2004 (Fig. 9). The previous wetlands changed into Gobi alkaline beach at present and the local ecosystems were greatly damaged (Zhang et al., 2013). Among the disappeared lake area of 540.0 km^2 in Xilin Gol from 1991 to 2009, Lake Wulagai accounted for 266 km^2 (49.3%). Since 2009, the lake showed remarkable fluctuation with rapid growth in 2012, then followed by a shrink since 2014 (Fig. 9).

3.4. Attribution analyses of lake changes in Inner Mongolia and Mongolia

The potential drivers of lake dynamics include both climate change and anthropogenic activities (L. Chen et al., 2014; Tao et al., 2015; Yigzaw and Hossain, 2016), here we used annual precipitation (AP), annual mean temperature (AMT) as measures of climatic factors, and coal mining, grazing, and irrigation as measures of human activities (Tao et al., 2015). We investigated the changing trends of these driving factors in the past 27 years for Inner Mongolia and Mongolia (Figs. 10 and 11). For precipitation, a decreasing trend before circa 2005 and an increasing trend after circa 2005 in AP have been observed for both Inner Mongolia (1991–2007: Slope = −4.83 mm/yr, $R^2 = 0.32$, $P = 0.018$; 2007–2015: Slope = 5.95 mm/yr, $R^2 = 0.15$, $P = 0.312$) and Mongolia (1991–2004: Slope = −4.77 mm/yr, $R^2 = 0.28$, $P = 0.013$; Slope = 3.61 mm/yr, 2004–2015: $R^2 = 0.27$, $P = 0.050$) (Fig. 10). For temperature, an increasing trend in AMT before 2007 has been found for both the two regions (Inner Mongolia: Slope = 0.06 °C/yr, $R^2 = 0.35$, $P = 0.197$; Mongolia: Slope = 0.06 °C/yr, $R^2 = 0.20$, $P = 0.013$) (Fig. 10), while significant fluctuations in AMT occurred after 2007. Coal mining increased dramatically in Inner Mongolia since 2000, from 72 million tons in 2000 to 1066 million tons in 2012 when the total coal mining reached its peak (Fig. 11). While coal mining in Mongolia was much lower compared to that in Inner Mongolia (Fig. 11). Generally, the grazing intensity in the two regions has increased during the period, and the grazing intensity in Inner Mongolia was more severe than that in Mongolia (Fig. 11). In the agricultural

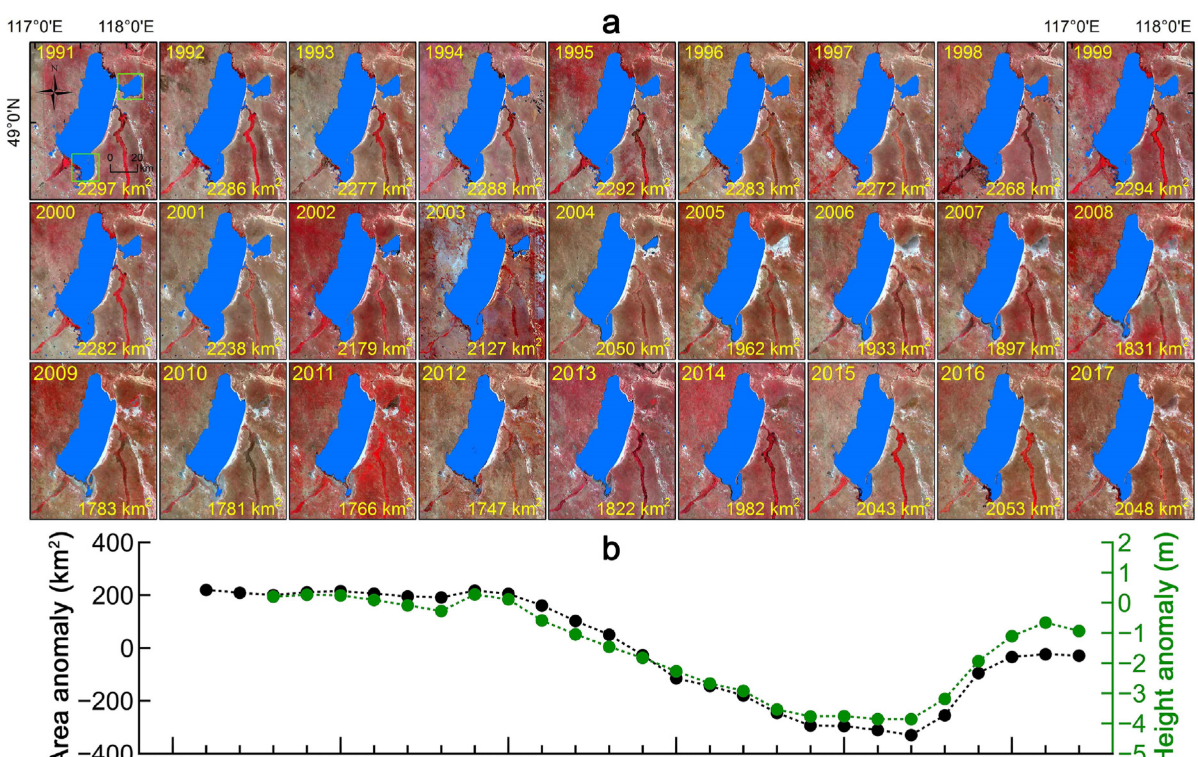

Fig. 8. Interannual variations in the spatial extent of Lake Hulun from 1991 to 2017. (a) For each subfigure, the base map was an RGB composite using bands NIR, Red, and Green of all available Landsat images with good-quality observations in the given year, while the yearly permanent water extent of Lake Hulun was overlapped on the base map. (b) Variations of area anomaly (1991–2017) and height anomaly (1993–2017) of Lake Hulun. (For interpretation of the references to colour in this figure legend, the reader is referred to the web version of this article.)

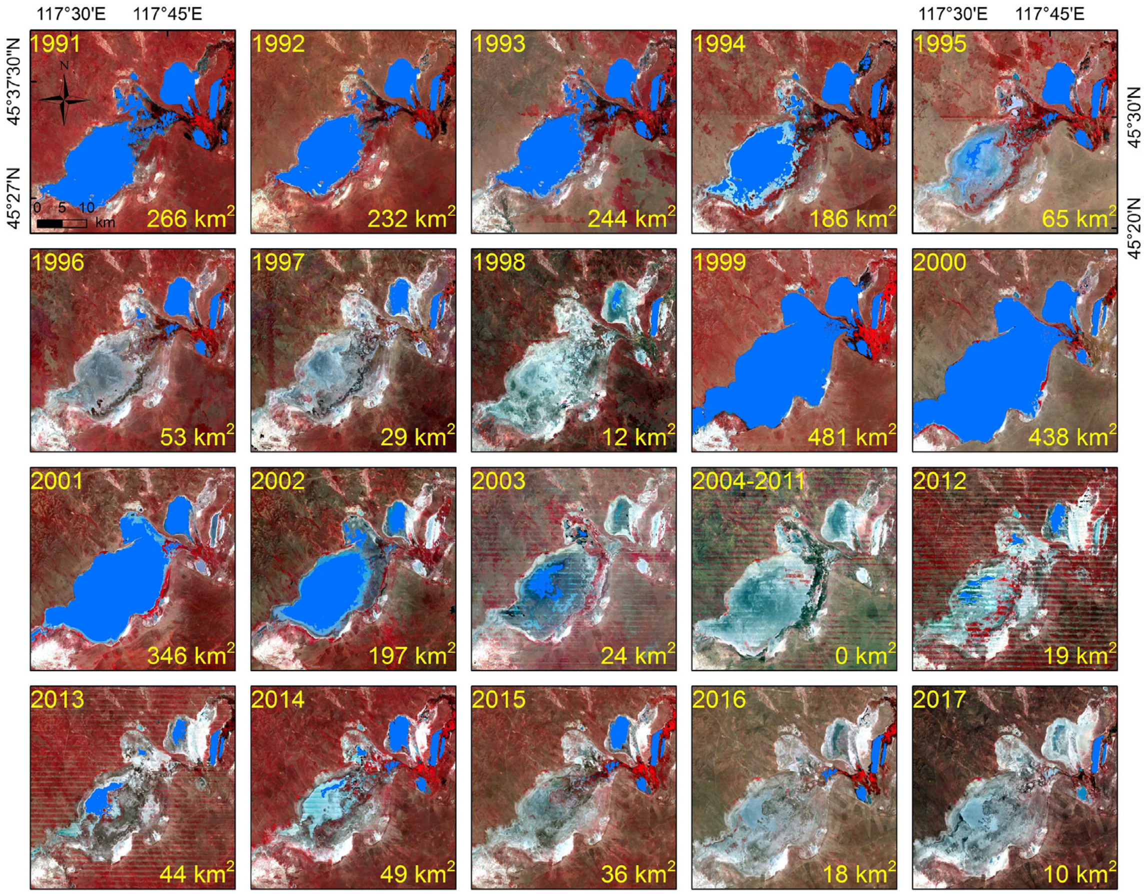

Fig. 9. Interannual variations in the spatial extent of Lake Wulagai from 1991 to 2017. For each subfigure, the base map was an RGB composite using bands NIR, Red, and Green of all available Landsat images with good-quality observations in the given year, and the yearly permanent water extent of Lake Wulagai was overlapped on the base map. (For interpretation of the references to colour in this figure legend, the reader is referred to the web version of this article.)

zone of Inner Mongolia, agricultural irrigation and water exploitation from groundwater and rivers might be another driver causing lake shrinking (Blanc et al., 2014; Tao et al., 2015). The area of irrigated croplands increased from 1.32 million ha in 1991 to 3.13 million ha in 2016 (Fig. 11). In the southeastern parts of Inner Mongolia, a large area of grasslands have been reclaimed into croplands (Dong et al., 2011), irrigation has rapidly depleted water resource of groundwater and rivers.

Considering the two stages of lake dynamics (lake shrinking during 1991–circa 2009 and lake recovery during circa 2009–2017) in both Inner Mongolia and Mongolia, here we conducted attribution analyses for both stages in the two regions. Due to the limitation of meteorological and socioeconomic data in the latter period, we extended the attribution analyses by using the 2006–2015 data to guarantee the reliability of statistical analyses. That was, we selected 1991–2009 and 2006–2015

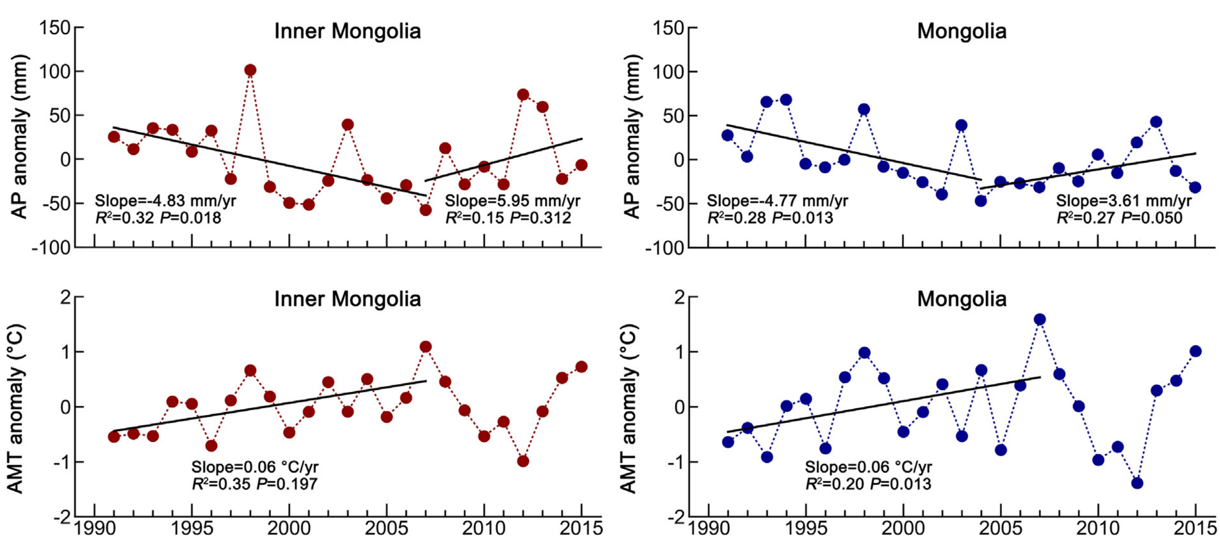

Fig. 10. Variation trends of annual precipitation (AP) and annual mean temperature (AMT) for Inner Mongolia and Mongolia from 1991 to 2015.

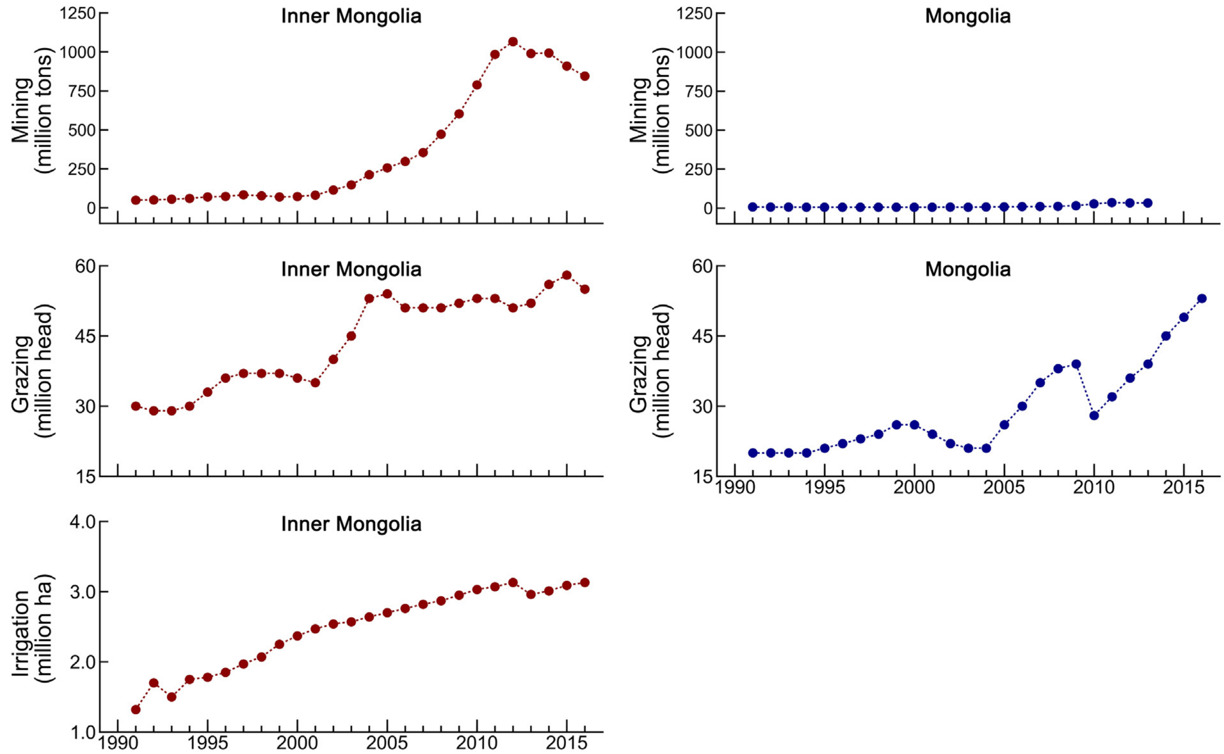

Fig. 11. Variation trends of coal mining (Mining), grazing intensity (Grazing), and irrigated croplands (Irrigation) area for Inner Mongolia and Mongolia from 1991 to 2016.

as the two periods to carry out the driver analyses of lake dynamics. We found the driving mechanisms were different across the two regions, and also different in the two periods (Table 2).

For Inner Mongolia, the grazing intensity and irrigation had statistically significant negative effects on lake areas and numbers from 1991 to 2009, respectively, while precipitation had significant positive effects (Table 2). From 2006 to 2015, precipitation had significant positive effects on lake areas and numbers, while the anthropogenic factors did not show any significant relationship with lake dynamics (Table 2). For Mongolia, the grazing intensity had significant negative effects on lake areas and numbers from 1991 to 2009, while precipitation had significant positive effects on lake numbers (Table 2). From 2006 to 2015, precipitation had significant positive effects on lake areas and numbers, while the anthropogenic factors also did not show any significant relationship with lake dynamics, the same with that in Inner Mongolia (Table 2).

As the main source of water supply for lakes, precipitation had positive effects on lake areas and numbers, which agree with the previous study (Tao et al., 2015). Here we analyzed the effects of precipitation on lake areas/numbers (Text S8, Figs. S9, S10, and 12). The peaks in lake areas and numbers in the Hulunbuir City and Xilin Gol League in 1999 matched the peaks of precipitation in 1998, which indicated the hysteresis of precipitation effects (Fig. 12). Also, the highest precipitation in the Hulunbuir City in 2013 and Xilin Gol League in 2012

Table 2

Multiple linear regression analyses of lake areas and numbers with climatic and anthropogenic driving factors in Inner Mongolia and Mongolia during the two periods of 1991–2009 and 2006–2015. For Inner Mongolia, the five dependent variables are annual precipitation (AP), annual mean temperature (AMT), coal mining production (Mining), Grazing, and Irrigation. For Mongolia, the four dependent variables are AP, AMT, Mining, and Grazing. R^2 is the proportion of variance in the dependent variable which can be explained by the selected explanatory variables. SEE is the standard error of the estimate. F and Sig. are the F-statistic and the p-value associated with it. For each linear regression, the variables that were not statistically significant ($P > 0.05$) were excluded.

Variables	Inner Mongolia				Mongolia			
	1991–2009		2006–2015		1991–2009		2006–2015	
	Areas	Numbers	Areas	Numbers	Areas	Numbers	Areas	Numbers
	Coef.	Coef.	Coef.	Coef.	Coef.	Coef.	Coef.	Coef.
AP	0.35	0.37	0.66	0.78		0.40	0.64	0.93
AMT								
Mining								
Grazing	−0.78				−0.71	−0.59		
Irrigation		−0.69						
Constant	4500	321	2066	−37	14,393	321	12,814	87
Model summary								
R^2	0.91	0.84	0.36	0.55	0.47	0.67	0.34	0.86
SEE	168	25	243	35	199	26	54	7
F	86.05	45.14	6.03	12.09	15.92	18.25	5.56	54.02
Sig.	0.000	0.000	0.04	0.008	0.001	0.000	0.046	0.000

contributed to the larger lake areas and numbers in the two regions in 2014 and 2013, respectively (Fig. 12). In terms of anthropogenic factors, overgrazing caused severe grassland degradation and subsequent decline in soil function and water conservation of grassland, thus, the lake water resource supply was affected. We found a more severe overgrazing in Inner Mongolia than that in Mongolia (Fig. 11), which agreed with the previous study (Tao et al., 2015). Irrigation directly consumed the water resource of groundwater and surface water (rivers or lakes) via a conveyance system. Depending on the type of conveyance system installed, part of the water withdrawal was lost through evaporation and/or seepage, and the water delivered at the field was either applied to crops directly or lost in the field distribution systems, thus had a negative effects on the lake water supply (Blanc et al., 2014; Takehiro et al., 2010; Tao et al., 2015). The irrigation kept increasing in Inner Mongolia especially in the period of 1991–2009 and then became relatively stable in the latter period (Fig. 11), while very limited irrigation existed in Mongolia.

Overall, both natural and anthropogenic factors significantly affected lake dynamics in Inner Mongolia and Mongolia before 2009, which agree with the previous studies (Tao et al., 2015; Liu et al., 2013). However, in this study, we found that in the recent decade precipitation played an increasingly important role for the recovery of lakes in the two regions since 2009.

Given the substantial spatial variations of lakes in Inner Mongolia, we further conducted attribution analyses of lake dynamics at the league level and the Hulunbuir City and Xilin Gol League were selected as the two regions dominating lake changes in Inner Mongolia. The results showed that lake dynamics were driven by varied factors in the two administrative regions during 1991–2009 and 2006–2015 (Table 3). Specifically, both natural and anthropogenic factors significantly affected lake dynamics in the Hulunbuir City and Xilin Gol League before 2009, while only precipitation dominated lake dynamics in the two administrative regions after 2009, which was consistent with the driver analyses results from the entire MP. For the Hulunbuir City, the grazing intensity and temperature had statistically significant negative effects on lake areas and numbers, coal mining had significant negative effects on lake areas from 1991 to 2009, while precipitation had positive effects on lake numbers (Table 3). From 2006 to 2015, precipitation had significant positive effects on lake areas and numbers, while the anthropogenic factors did not show any significant relationship with lake dynamics (Table 3). For the Xilin Gol League, coal mining had significant negative effects on lake numbers, while precipitation had significant positive effects on lake areas and numbers from 1991 to 2009 (Table 3). From 2006 to 2015, precipitation had significant positive effects on lake areas and numbers, while the anthropogenic factors also did not show any significant relationship with lake dynamics (Table 3). Such consistency between the driver analyses results from the entire MP and a municipal scale of the Hulunbuir City and Xilin Gol League proved that precipitation played an increasingly important role for the lake recovery on the MP after 2009. However, the new decrease in lake number and areas around 2014–2017 showed that anthropogenic influences cannot be ignored.

Given the dominant role of the major lakes in the regional variations of lake areas, we also analyzed the processes of two major lakes in Inner Mongolia. For Lake Hulun, the area shrink at the first stage could be related to the decrease in rainfall runoff and river water inflows (Li et al., 2018; Wang et al., 2013; Wang et al., 2012; Zhao et al., 2007), as well as the overgrazing and agriculture around the lake (Shen et al., 2006). Previous studies showed the inflows of the two rivers (the Kelulun River and Wuerxun River) decreased from 1.75 billion m^3 in 1999 to 0.25 billion m^3 in 2011 (Gao et al., 2017). The rapid expansion from 2013 to 2014 in the convex water body of the southern part of Lake Hulun (Fig. 8a) was consistent with the highest precipitation in the Hulunbuir City in 2013 (Fig. 12), which agreed with the previous study that the 2013 rainstorm attributed to the lake growth (Wan et al., 2016).

For Lake Wulagai, its water sources mainly rely on the recharge from the Wulagai River, the largest continental river in Inner Mongolia. However, the local government built the Wulagai Reservoir for fish-farming in the middle and upper reaches of the Wulagai River in 1977, and it cut off the water supply for Lake Wulagai and lead to continuous loss in lake area until 1998 (Tao et al., 2015; Zhang et al., 2013). Then, the dam of Wulagai Reservoir was destroyed by the flooding in 1998, the release of the reservoir water plus with the rainstorm in the Xilin Gol League caused the rapidly growing extent of Lake Wulagai in 1998–1999. Due to the huge water demand of the coal chemical industry, the local government rebuilt the Wulagai Reservoir in 2003 to provide water for the industrial parks nearby through the water diversion project (Tao et al., 2015). Without discharge of the Wulagai Reservoir, Lake Wulagai rapidly dried up and became a large saline alkaline beach since 2004 due to strong evaporation on the prairie (Li et al., 2013; Subuda et al., 2011). Thus, the remarkable variation of Lake Wulagai (Fig. 9) was strongly affected by the reservoir building related to the coal mining industry, agreed with our attribution analyses in Xilin Gol (Table 3).

3.5. Uncertainty and implications for future studies

In this study, we systematically discussed the inter-annual dynamics of lakes, while the intra-annual lake variations could also be remarkable in the arid and semi-arid Mongolian Plateau which was not highlighted in this study. Here we took nine typical lakes in different precipitation

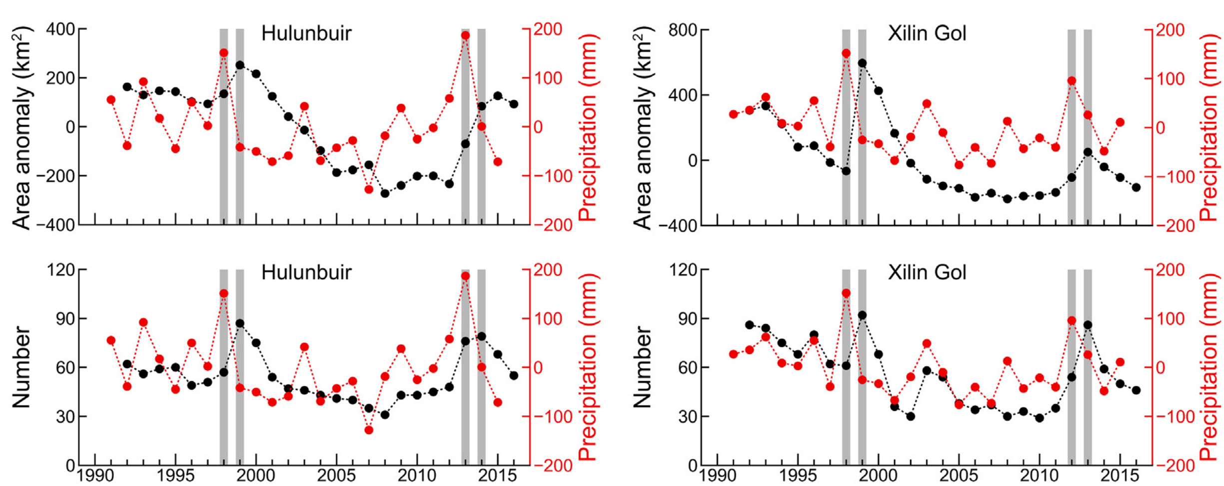

Fig. 12. Variations of lake areas and numbers (1992–2016), and precipitation (1991–2015) in the Hulunbuir City and Xilin Gol League of Inner Mongolia.

Table 3
Multiple linear regression analyses of lake areas and numbers with climatic and anthropogenic driving factors in the Hulunbuir City and Xilin Gol League of Inner Mongolia during the two periods of 1991–2009 and 2006–2015. For the two administrative regions, the four dependent variables are annual precipitation (AP), annual mean temperature (AMT), coal mining production (Mining), and Grazing. R^2 is the proportion of variance in the dependent variable which can be explained by the selected explanatory variables. SEE is the standard error of the estimate. F and Sig. are the F-statistic and the p-value associated with it. For each linear regression, the variables that were not statistically significant ($P > 0.05$) were excluded.

Variables	Hulunbuir				Xilin Gol			
	1991–2009		2006–2015		1991–2009		2006–2015	
	Areas	Numbers	Areas	Numbers	Areas	Numbers	Areas	Numbers
	Coef.	Coef.	Coef.	Coef.	Coef.	Coef.	Coef.	Coef.
AP		0.40	0.65	0.81	0.61	0.64	0.78	0.78
AMT	−0.16	−0.33						
Mining	−0.46					−0.39		
Grazing	−0.57	−0.52						
Constant	2765	83	1776	−19	−314	−2	−149	−21
Model summary								
R^2	0.93	0.67	0.36	0.61	0.33	0.62	0.56	0.57
SEE	43	8	110	11	205	13	64	12
F	79.43	12.61	5.97	15.34	9.29	15.02	12.22	12.79
Sig.	0.000	0.000	0.04	0.004	0.008	0.000	0.008	0.007

gradients/sub-zones in Inner Mongolia for an example, the intra-annual variations of water extent in 2016–2017 were investigated by using all the available Landsat ETM+/OLI observations. Considering the freezing of lake water during November–March, we only took the lake variations during April–October into consideration. The results showed that the lakes in different sub-zones had different patterns of intra-annual variations (Fig. S11). This suggested the importance of the information of intra-annual lake variations in understanding the dynamics of lakes, especially in such a typical region sensitive to climate change like the MP. Fortunately, the launch of Sentinel-2 in 2015 greatly enhanced the frequency of earth observations with medium spatial resolution, facilitating the monitoring of intra-annual lake variations in future studies.

In addition, this study focused on the lakes over 1 km^2 on the MP from 1991 to 2017. However, previous study proposed that the smaller lakes <1 km^2 could be more vulnerable to climate change (Zou et al., 2017), and could also play an important role in the local ecosystems such as their large contribution to CO_2 and CH_4 emissions (Holgerson and Raymond, 2016). Therefore, the knowledge of the continuous dynamics of these lakes in such an arid and semi-arid region like MP is significant to global change researches and deserves more attention in future studies.

4. Conclusions

As important water sources of agricultural and industrial production as well as human livelihood, lake dynamics would lead to a series of consequences on the environment and terrestrial ecosystems on the MP. Based on the Landsat-based annual water body maps generated in this study, we investigated the interannual dynamics of lakes in terms of both lake area and numbers on the plateau. We found the lake areas and numbers of both Inner Mongolia and Mongolia experienced decreasing trends from 1991 to circa 2009, then followed by a recovered lake increase since 2009. Lake variations of Inner Mongolia were stronger than that of Mongolia, which was indicated by the larger change rates in both lake areas and numbers. Moreover, we found both climatic and socioeconomic factors affected the lake dynamics on the MP before the turning point (the year of 2009), while precipitation played an increasingly important role for the lake recovery process after 2009. We also found that the lake dynamics in both Inner Mongolia and Mongolia were dominated by limited administrative regions, i.e., the Hulunbuir and Xilin Gol leagues in Inner Mongolia while the Ubsa Aymag in Mongolia, or more specifically Lake Hulun and Lake Wulagai in Inner Mongolia and a couple of lakes in Mongolia. This study suggested the key for lake management and treatment as well as adaption to climate change is to consider the major lakes as a priority.

Acknowledgements

This study is funded by the Strategic Priority Research Program (XDA19040301) and Key Research Program of Frontier Sciences (QYZDB-SSW-DQC005) of Chinese Academy of Sciences (CAS), and the "Thousand Youth Talents Plan". We thank Zhiqi Yang, Nanshan You, and Rui Zhao for their valuable comments during the study. We acknowledge the Joint Research Center (JRC) of European Commission for making the water body maps available (https://global-surface-water.appspot.com/). The CRU TS V4.01 climate data are available through the Climatic Research Unit (http://www.cru.uea.ac.uk/data/). The socioeconomic data for Inner Mongolia and Mongolia is from Statistical Year Book, the United States Energy Information Administration (http://www.indexmundi.com), and the FAOSTAT (http://faostat.fao.org).

Appendix A. Supplementary data

Supplementary data to this article can be found online at https://doi.org/10.1016/j.scitotenv.2019.06.341.

References

Bao, G., Qin, Z., Bao, Y., Zhou, Y., Li, W., Sanjjav, A., 2014. NDVI-based long-term vegetation dynamics and its response to climatic change in the Mongolian Plateau. Remote Sens. 6, 8337–8358. https://doi.org/10.3390/rs6098337.
Blanc, E., Strzepek, K., Schlosser, A., Jacoby, H., Gueneau, A., Fant, C., Rausch, S., Reilly, J., 2014. Modeling U.S. water resources under climate change. Earth's Future 2, 197–224. https://doi.org/10.1002/2013EF000214.
Buchroithner, M., Bolch, T., 2015. Glacier Lake Outburst Floods (GLOFs) - Mapping the Hazard of a Threat to High Asia and Beyond, Impact of Global Changes on Mountains.
Cai, Z., Jin, T., Li, C., Ofterdinger, U., Zhang, S., Ding, A., Li, J., 2016. Is China's fifth-largest inland lake to dry-up? Incorporated hydrological and satellite-based methods for forecasting Hulun lake water levels. Adv. Water Resour. 94, 185–199. https://doi.org/10.1016/j.advwatres.2016.05.010.
Chander, G., Markham, B.L., Helder, D.L., 2009. Summary of current radiometric calibration coefficients for Landsat MSS, TM, ETM+, and EO-1 ALI sensors. Remote Sens. Environ. 113, 893–903. https://doi.org/10.1016/j.rse.2009.01.007.
Chang, B., Li, R., Zhu, C., Liu, K., 2015. Quantitative impacts of climate change and human activities on water-surface area variations from the 1990s to 2013 in Honghu Lake, China. Water 7, 2881–2899. https://doi.org/10.3390/w7062881.
Chen, X., Chuai, X., Yang, L., Zhao, H., 2012. Climatic warming and overgrazing induced the high concentration of organic matter in Lake Hulun, a large shallow eutrophic steppe lake in northern China. Sci. Total Environ. 431, 332. https://doi.org/10.1016/j.scitotenv.2012.05.052.
Chen, J., John, R., Zhang, Y., Shao, C., Brown, D.G., Batkhishig, O., Amarjargal, A., Ouyang, Z., Dong, G., Wang, D., 2014. Divergences of two coupled human and natural systems on the Mongolian Plateau. Bioscience 65, 559–570. https://doi.org/10.1093/biosci/biv050.
Chen, L., Michishita, R., Xu, B., 2014. Abrupt spatiotemporal land and water changes and their potential drivers in Poyang Lake, 2000–2012. ISPRS J. Photogramm. Remote Sens. 98, 85–93. https://doi.org/10.1016/j.isprsjprs.2014.09.014.

Chen, F., Zhang, M.M., Tian, B.S., Li, Z., 2017. Extraction of glacial lake outlines in Tibet Plateau using Landsat 8 imagery and Google Earth Engine. IEEE J. Sel. Top. Appl. Earth Obs. Remote Sens. 10, 4002–4009. https://doi.org/10.1109/Jstars.2017.2705718.
Chen, B., Chen, L.F., Huang, B., Michishita, R., Xu, B., 2018. Dynamic monitoring of the Poyang Lake wetland by integrating Landsat and MODIS observations. ISPRS J. Photogramm. Remote Sens. 139, 75–87. https://doi.org/10.1016/j.isprsjprs.2018.02.021.
Crétaux, J.F., Jelinski, W., Calmant, S., Kouraev, A., Vuglinski, V., Bergé-Nguyen, M., Gennero, M.C., Nino, F., Rio, R.A.D., Cazenave, A., 2011. SOLS: a lake database to monitor in the Near Real Time water level and storage variations from remote sensing data. Adv. Space Res. 47, 1497–1507. https://doi.org/10.1016/j.asr.2011.01.004.
Dong, J., Liu, J., Yan, H., Tao, F., Kuang, W., 2011. Spatio-temporal pattern and rationality of land reclamation and cropland abandonment in mid-eastern Inner Mongolia of China in 1990–2005. Environ. Monit. Assess. 179, 137.
Dwyer, J.L., Roy, D.P., Sauer, B., Jenkerson, C.B., Zhang, H.K.K., Lymburner, L., 2018. Analysis Ready Data: enabling analysis of the Landsat archive. Remote Sens. 10. https://doi.org/10.3390/rs10091363.
Feyisa, G.L., Meilby, H., Fensholt, R., Proud, S.R., 2014. Automated water extraction index: a new technique for surface water mapping using Landsat imagery. Remote Sens. Environ. 140, 23–35. https://doi.org/10.1016/j.rse.2013.08.029.
Fisher, A., Flood, N., Danaher, T., 2016. Comparing Landsat water index methods for automated water classification in eastern Australia. Remote Sens. Environ. 175, 167–182. https://doi.org/10.1016/j.rse.2015.12.055.
Gao, H., Ryan, M.C., Li, C., Sun, B., 2017. Understanding the role of groundwater in a remote transboundary lake (Hulun Lake, China). Water 9, 363. https://doi.org/10.3390/w9050363.
Gorelick, N., Hancher, M., Dixon, M., Ilyushchenko, S., Thau, D., Moore, R., 2017. Google Earth Engine: planetary-scale geospatial analysis for everyone. Remote Sens. Environ. 202, 18–27. https://doi.org/10.1016/j.rse.2017.06.031.
Han, X., Feng, L., Hu, C., Chen, X., Han, X., Feng, L., Hu, C., Chen, X., 2017. Wetland changes of China's largest freshwater lake and their linkage with the Three Gorges Dam. Remote Sens. Environ. 204, 799–811. https://doi.org/10.1016/j.rse.2017.09.023.
Hansen, M.C., Loveland, T.R., 2012. A review of large area monitoring of land cover change using Landsat data. Remote Sens. Environ. 122, 66–74. https://doi.org/10.1016/j.rse.2011.08.024.
Holgerson, M.A., Raymond, P.A., 2016. Large contribution to inland water CO2 and CH4 emissions from very small ponds. Nat. Geosci. 9, 222–U150. https://doi.org/10.1038/NGEO2654.
Hou, X., Feng, L., Duan, H., Chen, X., Sun, D., Shi, K., 2017. Fifteen-year monitoring of the turbidity dynamics in large lakes and reservoirs in the middle and lower basin of the Yangtze River, China. Remote Sens. Environ. 190, 107–121. https://doi.org/10.1016/j.rse.2016.12.006.
Hou, X.J., Feng, L., Chen, X.L., Zhang, Y.L., 2018. Dynamics of the wetland vegetation in large lakes of the Yangtze Plain in response to both fertilizer consumption and climatic changes. ISPRS J. Photogramm. Remote Sens. 141, 148–160. https://doi.org/10.1016/j.isprsjprs.2018.04.015.
Huang, C., Chen, Y., Zhang, S., Wu, J., 2018. Detecting, extracting and monitoring surface water from space using optical sensors—a review. Rev. Geophys. 56, 333–360. https://doi.org/10.1029/2018RG000598.
John, R., Chen, J., Ouyang, Z.T., Xiao, J., Becker, R., Samanta, A., Ganguly, S., Yuan, W., Batkhishig, O., 2013. Vegetation response to extreme climate events on the Mongolian Plateau from 2000 to 2010. Environ. Res. Lett. 8, 035033. https://doi.org/10.1088/1748-9326/8/3/035033.
John, R., Chen, J., Giannico, V., Park, H., Xiao, J., Shirkey, G., Ouyang, Z., Shao, C., Lafortezza, R., Qi, J., 2018. Grassland canopy cover and aboveground biomass in Mongolia and Inner Mongolia: spatiotemporal estimates and controlling factors. Remote Sens. Environ. 213, 34–48. https://doi.org/10.1016/j.rse.2018.05.002.
Ju, J., Roy, D.P., 2008. The availability of cloud-free Landsat ETM+ data over the conterminous United States and globally. Remote Sens. Environ. 112, 1196–1211.
Ke, C.Q., 2016. Monitoring changes in the water volume of Hulun Lake by integrating satellite altimetry data and Landsat images between 1992 and 2010. J. Appl. Remote. Sens. 10, 016029.
Li, S., Ferguson, D.K., Wang, Y., Jinfeng, L.I., Yao, J., 2013. Climate reconstruction based on pollen analysis in Inner Mongolia, North China from 51.9 to 30.6 kaBP. Acta Geol. Sin. 87, 1444–1459.
Li, H., Gao, Y., Li, Y., Yan, S., Xu, Y., Li, H., Gao, Y., Li, Y., Yan, S., Xu, Y., 2017. Dynamic of Dalinor Lakes in the Inner Mongolian Plateau and its driving factors during 1976–2015. Water 9, 749. https://doi.org/10.3390/w9100749.
Li, C., Wang, J., Hu, R., Yin, S., Bao, Y., Li, Y., 2018. ICESat/GLAS-derived changes in the water level of Hulun Lake, Inner Mongolia, from 2003 to 2009. Front. Earth Sci. China 12, 420–430. https://doi.org/10.1007/s11707-017-0666-8.
Liu, H., Yin, Y., Piao, S., Zhao, F., Engels, M., Ciais, P., 2013. Disappearing lakes in semiarid Northern China: drivers and environmental impact. Environ. Sci. Technol. 47, 12107–12114. https://doi.org/10.1021/es305298q.
Liu, J., Yang, H., Gosling, S.N., Kummu, M., Flörke, M., Pfister, S., Hanasaki, N., Wada, Y., Zhang, X., Zheng, C., 2017. Water scarcity assessments in the past, present, and future. Earth's Future 5, 545–559. https://doi.org/10.1002/2016EF000518.
Lu, S.L., Wu, B.F., Yan, N.N., Wang, H., 2011. Water body mapping method with HJ-1A/B satellite imagery. Int. J. Appl. Earth Obs. Geoinf. 13, 428–434. https://doi.org/10.1016/j.jag.2010.09.006.
Lü, C., Bing, W., Jiang, H., Vogt, R.D., Zhou, B., Rui, G., Le, Z., Wang, W., Xie, Z., Wang, J., 2016. Responses of organic phosphorus fractionation to environmental conditions and lake evolution. Environ. Sci. Technol. 50, 5007–5016. https://doi.org/10.1021/acs.est.5b05057.
Ma, R., Duan, H., Hu, C., Feng, X., Li, A., Ju, W., Jiang, J., Yang, G., 2010. A half-century of changes in China's lakes: global warming or human influence? Geophys. Res. Lett. 37. https://doi.org/10.1029/2010GL045514.
McFeeters, S.K., 1996. The use of the normalized difference water index (NDWI) in the delineation of open water features. Int. J. Remote Sens. 17, 1425–1432. https://doi.org/10.1080/01431169608948714.
Nyland, K.E., Gunn, G.E., Shiklomanov, N.I., Engstrom, R.N., Streletskiy, D.A., 2018. Land cover change in the Lower Yenisei River using dense stacking of Landsat imagery in Google Earth Engine. Remote Sens. 10. https://doi.org/10.3390/rs10081226.
O'Reilly, C.M., Sharma, S., Gray, D.K., Hampton, S.E., Read, J.S., Rowley, R.J., Schneider, P., Lenters, J.D., Mcintyre, P.B., Kraemer, B.M., 2015. Rapid and highly variable warming of lake surface waters around the globe. Geophys. Res. Lett. 42. https://doi.org/10.1002/2015GL066235.
Patel, N.N., Angiuli, E., Gamba, P., Gaughan, A., Lisini, G., Stevens, F.R., Tatem, A.J., Trianni, G., 2015. Multitemporal settlement and population mapping from Landsat using Google Earth Engine. Int. J. Appl. Earth Obs. Geoinf. 35, 199–208. https://doi.org/10.1016/j.jag.2014.09.005.
Pekel, J.F., Cottam, A., Gorelick, N., Belward, A.S., 2016. High-resolution mapping of global surface water and its long-term changes. Nature 540, 418–422. https://doi.org/10.1038/nature20584.
Rokni, K., Ahmad, A., Solaimani, K., Hazini, S., 2015. A new approach for surface water change detection: integration of pixel level image fusion and image classification techniques. Int. J. Appl. Earth Obs. Geoinf. 34, 226–234. https://doi.org/10.1016/j.jag.2014.08.014.
Sha, Y., Shi, Z., Liu, X., An, Z., 2015. Distinct impacts of the Mongolian and Tibetan Plateaus on the evolution of the East Asian monsoon. J. Geophys. Res. Atmos. 120, 4764–4782. https://doi.org/10.1002/2014JD022880.
Shen, J.G., Bai, M.L., Yun peng, L.I., 2006. Influence of climatic change and humanity activities on ecological environment in eastern area of Inner Mongolia. Journal of Natural Disasters 15, 84–91. https://doi.org/10.3969/j.issn.1004-4574.2006.06.015.
Song, C., Huang, B., Ke, L., 2013. Modeling and analysis of lake water storage changes on the Tibetan Plateau using multi-mission satellite data. Remote Sens. Environ. 135, 25–35. https://doi.org/10.1016/j.rse.2013.03.013.
Song, C.Q., Huang, B., Ke, L.H., Richards, K.S., 2014. Remote sensing of alpine lake water environment changes on the Tibetan Plateau and surroundings: a review. ISPRS J. Photogramm. Remote Sens. 92, 26–37. https://doi.org/10.1016/j.isprsjprs.2014.03.001.
Subuda, Y. I. Jin, J. Q. Chen, X. X. Bao, and Sanasiqin, 2011. Analysis of vegetation degeneration succession trend in middle and lower reaches of Wulagai Wetland of Inner Mongolia. Chinese Journal of Grassland.
Takehiro, S., Tomoo, O., Undarmaa, J., Kazuhiko, T., 2010. Threshold changes in vegetation along a grazing gradient in Mongolian rangelands. J. Ecol. 96, 145–154. https://doi.org/10.1111/j.1365-2745.2007.01315.x.
Tao, S., Fang, J., Zhao, X., Zhao, S., Shen, H., Hu, H., Tang, Z., Wang, Z., Guo, Q., 2015. Rapid loss of lakes on the Mongolian Plateau. PNAS 112, 2281–2286. https://doi.org/10.1073/pnas.1411748112.
Wan, H.W., Kang, J., Shuai, G., Shen, W.M., 2016. Study on dynamic change of Hulun Lake water area and climate driving force analysis. China Environ. Sci. 36.
Wang, Z., Changyou, L.I., Zhang, S., Jia, K.A., Weiping, L.I., 2012. Hydrological changes in Lake Hulun based on water balance model. J. Lake Sci. 24, 667–674. https://doi.org/10.18307/2012.0504.
Wang, X., Gong, P., Zhao, Y., Xu, Y., Cheng, X., Niu, Z., Luo, Z., Huang, H., 2013. Water-level changes in China's large lakes determined from ICESat/GLAS data. Remote Sens. Environ. 132, 131–144. https://doi.org/10.1016/j.rse.2013.01.005.
Wang, R., Peng, W., Liu, X., Wu, W., Chen, X., Zhang, S., 2018. Responses of water level in China's largest freshwater lake to the meteorological drought index (SPEI) in the past five decades. Water 10, 137. https://doi.org/10.3390/w10020137.
Wulder, M.A., Coops, N.C., 2014. Make Earth observations open access. Nature 513, 30–31. https://doi.org/10.1038/513030a.
Wulder, M.A., White, J.C., Loveland, T.R., Woodcock, C.E., Belward, A.S., Cohen, W.B., Fosnight, E.A., Shaw, J., Masek, J.G., Roy, D.P., 2016. The global Landsat archive: status, consolidation, and direction. Remote Sens. Environ. 185, 271–283. https://doi.org/10.1016/j.rse.2015.11.032.
Xu, H.Q., 2006. Modification of normalised difference water index (NDWI) to enhance open water features in remotely sensed imagery. Int. J. Remote Sens. 27, 3025–3033. https://doi.org/10.1080/01431160600589179.
Yamazaki, D., Trigg, M.A., Ikeshima, D., 2015. Development of a global ~90m water body map using multi-temporal Landsat images. Remote Sens. Environ. 171, 337–351. https://doi.org/10.1016/j.rse.2015.10.014.
Yigzaw, W., Hossain, F., 2016. Water sustainability of large cities in the United States from the perspectives of population increase, anthropogenic activities, and climate change. Earth's Future 4, 603–617. https://doi.org/10.1002/2016EF000393.
Yu, Z., Liu, X., Wang, Y., Chi, Z., Wang, X., Lan, H., 2014. A 48.5-ka climate record from Wulagai Lake in Inner Mongolia, Northeast China. Quat. Int. 333, 13–19. https://doi.org/10.1016/j.quaint.2014.04.006.
Zhang, G., Xie, H., Kang, S., Yi, D., Ackley, S.F., 2011. Monitoring lake level changes on the Tibetan Plateau using ICESat altimetry data (2003–2009). Remote Sens. Environ. 115, 1733–1742. https://doi.org/10.1016/j.rse.2011.03.005.
Zhang, B., Song, X., Ying, M.A., Hongmei, B.U., 2013. Impact of coal power base constructions on the environment around the Wulagai water reservoir, Xilinguole, Inner Mongolia. Journal of Arid Land Resources & Environment 719-720, 924–928. https://doi.org/10.13448/j.cnki.jalre.2013.01.016.
Zhang, G., Yao, T., Piao, S., Bolch, T., Xie, H., Chen, D., Gao, Y., O'Reilly, C.M., Shum, C.K., Yang, K., 2017. Extensive and drastically different alpine lake changes on Asia's high plateaus during the past four decades. Geophys. Res. Lett. 44. https://doi.org/10.1002/2016GL072033.
Zhao, H., Li, C., Zhao, H., Tian, H., Song, Q., Dou, Z., 2007. The climate change and its effect on the water environment in the Hulun Lake Wetland. J. Glaciol. Geocryol. 29, 795–801. https://doi.org/10.3969/j.issn.1000-0240.2007.05.018.

Zhu, Z., Woodcock, C.E., 2014. Automated cloud, cloud shadow, and snow detection in multitemporal Landsat data: an algorithm designed specifically for monitoring land cover change. Remote Sens. Environ. 152, 217–234. https://doi.org/10.1016/j.rse.2014.06.012.

Zou, Z., Dong, J., Menarguez, M.A., Xiao, X., Qin, Y., Doughty, R.B., Hooker, K.V., David, H.K., 2017. Continued decrease of open surface water body area in Oklahoma during 1984–2015. Sci. Total Environ. 595, 451–460. https://doi.org/10.1016/j.scitotenv.2017.03.259.

Zou, Z., Xiao, X., Dong, J., Qin, Y., Doughty, R.B., Menarguez, M.A., Zhang, G., Wang, J., 2018. Divergent trends of open-surface water body area in the contiguous United States from 1984 to 2016. PNAS 115, 3810–3815. https://doi.org/10.1073/pnas.1719275115.

Zurqani, H.A., Post, C.J., Mikhailova, E.A., Schlautman, M.A., Sharp, J.L., 2018. Geospatial analysis of land use change in the Savannah River Basin using Google Earth Engine. Int. J. Appl. Earth Obs. Geoinf. 69, 175–185. https://doi.org/10.1016/j.jag.2017.12.006.